



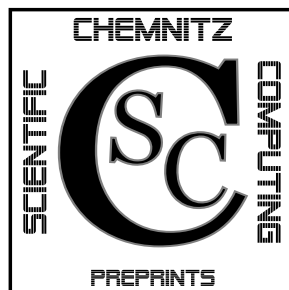
TECHNISCHE UNIVERSITÄT CHEMNITZ

Arnd Meyer

Rolf Springer

Basics of Linear Thermoelasticity

CSC/15-03



Chemnitz Scientific Computing  
Preprints

**Impressum:**

**Chemnitz Scientific Computing Preprints** — ISSN 1864-0087

(1995–2005: Preprintreihe des Chemnitzer SFB393)

**Herausgeber:**

Professuren für  
Numerische und Angewandte Mathematik  
an der Fakultät für Mathematik  
der Technischen Universität Chemnitz

**Postanschrift:**

TU Chemnitz, Fakultät für Mathematik  
09107 Chemnitz

**Sitz:**

Reichenhainer Str. 41, 09126 Chemnitz

<http://www.tu-chemnitz.de/mathematik/csc/>



**TECHNISCHE UNIVERSITÄT CHEMNITZ**  
Chemnitz Scientific Computing  
Preprints

Arnd Meyer

Rolf Springer

Basics of Linear Thermoelasticity

CSC/15-03

This work was performed within the Federal Cluster of Excellence EXC 1075 “MERGE Technologies for Multifunctional Lightweight Structures” and supported by the German Research Foundation (DFG). Financial support is gratefully acknowledged.



# Contents

<b>1. Introduction</b>	<b>1</b>
1.1. Notation . . . . .	1
1.2. Differential geometry . . . . .	2
<b>2. Theoretical Background</b>	<b>3</b>
2.1. Problem setting . . . . .	3
2.2. Linear elasticity . . . . .	4
2.3. Linear thermoelasticity . . . . .	4
2.4. Heat equation . . . . .	5
<b>3. Special Cases of Linear Thermoelasticity</b>	<b>5</b>
3.1. Isotropic material . . . . .	5
3.2. Transversely isotropic material . . . . .	6
<b>4. Weak Formulation</b>	<b>8</b>
<b>5. Implementation</b>	<b>10</b>
<b>6. Numerical Examples</b>	<b>12</b>
6.1. Comparison of the results in the isotropic case . . . . .	12
6.2. Test of the thermal behaviour . . . . .	13
6.3. Comparison with “Abaqus” . . . . .	14
<b>A. Results of the Computation</b>	<b>19</b>
A.1. Comparison of the results in the isotropic case . . . . .	19
A.2. Test of the thermal behaviour . . . . .	22
A.3. Results of A3D-TEAni in the comparison computation . . . . .	24

Author’s addresses:

Arnd Meyer  
Rolf Springer  
TU Chemnitz  
Fakultät für Mathematik  
D-09107 Chemnitz

<http://www.tu-chemnitz.de/mathematik/>

# 1. Introduction

This work was written in the framework of the “Cluster of Excellence Merge”. The goal of this cluster is to create lightweight structures with different abilities, for example integrated sensors. Nevertheless, these structures have to fulfill some mechanical requirements, besides these additional abilities.

Therefore it is necessary to simulate these structures and their behaviour under mechanical and thermal loads. For this simulation a mathematical description of the structure-properties is needed. This work is one first step on the way of describing the properties of such complex structures.

For this purpose the mathematical description of the behaviour of material in the case of linear thermoelasticity is investigated in this paper. At first, this is done, by increasing the case of linear elasticity by adding the thermal behaviour of the material in a very general way. Afterwards, this general setting is restricted to two special cases and some numerical results for both cases will be represented.

## 1.1. Notation

In the following chapters different types of tensors will occur. For better understanding of the following sections we use nearly strict different types of letters for those different types of tensors.

In this work, small Greek letters are used for scalar values and small boldface Latin letters for tensors of first order. In addition, we use bold and capitalised Latin letters for tensors of second order, and big, fractured letters for tensors of fourth order. An overview of these rules is given in table 1. Moreover,  $\mathcal{T}_1$  stands for the space of first order tensors, which are the vector functions over a given domain  $\Omega$ ,  $\mathcal{T}_2$  stands for the space of second order tensor fields and so on.

$\alpha \in \mathcal{T}_0$	scalar function:	$\mathbb{R}^3 \supset \Omega \rightarrow \mathbb{R}$
$\mathbf{a} \in \mathcal{T}_1$	tensorfield of first order:	$\mathbb{R}^3 \supset \Omega \rightarrow \mathbb{R}^3$
$\mathbf{A} \in \mathcal{T}_2$	tensorfield of second order:	linear mappings: $\mathcal{T}_1 \rightarrow \mathcal{T}_1$
$\mathfrak{A} \in \mathcal{T}_4$	tensorfield of fourth order:	linear mappings: $\mathcal{T}_2 \rightarrow \mathcal{T}_2$

Table 1: Notation in this work

This rules are only nearly strict, because there are some exceptions in this work. The reason for this exceptions are some widely accepted names in mechanical literature. Therefore, we will use this names for a better understanding of the following chapters, although they are against the notation explained in table 1. This exceptions are in table 2.

Additional to this notation remarks for naming tensors, there will be some remarks for tensor operations. The symbol “ $\otimes$ ” for the product of two tensors is suppressed in

$\varepsilon$	linearised strain tensor (tensor of second order, see section 2.2)
$\sigma$	Cauchy stress tensor (tensor of second order, see section 2.1)
$\kappa$	heat conduction tensor (tensor of second order, see section 2.4)
$\mathbf{X}$	point of the reference configuration (see section 2.1)
$\mathbf{G}_i$	covariant basis (see (1))
$\mathbf{G}^i$	contravariant basis (see (2))

Table 2: Exceptions from table 1

this work, i.e. for two tensors  $\mathbf{a}, \mathbf{b}$  the tensor product will be written as “ $\mathbf{ab}$ ” instead of “ $\mathbf{a} \otimes \mathbf{b}$ ”. Moreover, the inner product of two tensors  $\mathbf{a}$  and  $\mathbf{b}$  will be written as  $\mathbf{a} \cdot \mathbf{b}$  and the double contraction of two tensors  $\mathbf{A}, \mathbf{B}$  of at least second order will be denoted by “ $\mathbf{A} : \mathbf{B}$ ”.

## 1.2. Differential geometry

We are looking on a parametrised set  $\Omega \subset \mathbb{R}^3$ , which is given by

$$\Omega = \left\{ \mathbf{X}(\eta^1, \eta^2, \eta^3) \mid (\eta^1, \eta^2, \eta^3) \in \mathcal{P} \subset \mathbb{R}^3 \right\}.$$

Here,  $\mathbf{X} : \mathcal{P} \rightarrow \mathbb{R}^3$  is a function, which describes the points of  $\Omega$ ,  $\mathcal{P}$  is the parameter set and  $\eta^i$  ( $i = 1, 2, 3$ ) are the parameters.

For this parametrisation we can define the, so called, **covariant basis** by

$$\mathbf{G}_i = \frac{\partial}{\partial \eta^i} \mathbf{X}, \quad (1)$$

and the **contravariant basis** by

$$\mathbf{G}_i \cdot \mathbf{G}^j = \delta_i^j, \quad (2)$$

where  $\delta_i^j$  is given by

$$\delta_i^j = \begin{cases} 1 & \text{if } i = j \\ 0 & \text{if } i \neq j \end{cases}.$$

With the help of these tensors of first order two operators can be defined by

$$\begin{aligned} \text{Grad} &:= \mathbf{G}^j \frac{\partial}{\partial \eta^j} \\ \text{Div} &:= \text{Grad} \cdot, \end{aligned} \quad (3)$$

where  $\text{Grad} \cdot$  is defined by

$$\text{Div} \mathbf{v} = \text{Grad} \cdot \mathbf{v} = \mathbf{G}^j \cdot \frac{\partial}{\partial \eta^j} \mathbf{v} =: \mathbf{G}^j \cdot \mathbf{v}_{,j}, \quad (4)$$

for  $\mathbf{v} \in (\mathbb{H}^1(\Omega))^3$ . Note that from now on, as well as in the equations (3) and (4), the **Einstein summation convention** is used. This means that all indices, which are occurring twice, imply the summation from one to three.

Furthermore, for two tensors  $\mathbf{A}, \mathbf{B} \in \mathcal{T}_2$  the double contraction is the trace of the dot product of  $\mathbf{A}$  and  $\mathbf{B}$ , i.e.

$$\mathbf{A} : \mathbf{B} = \text{tr}(\mathbf{A} \cdot \mathbf{B}) = \text{tr}(\mathbf{B} \cdot \mathbf{A}).$$

## 2. Theoretical Background

In this chapter we will give a short introduction in the theory of linear thermoelasticity. Therefore, in the next section the general problem setting is introduced. In section 2.2 the theory of linear elasticity is shortly explained, in section 2.3 this theory is expanded to the case of thermoelasticity, and section 2.4 concerns the heat equation.

### 2.1. Problem setting

The parametrised set  $\Omega \subset \mathbb{R}^3$  from section 1.2, described by

$$\Omega = \left\{ \mathbf{X}(\eta^1, \eta^2, \eta^3) \mid (\eta^1, \eta^2, \eta^3) \in \mathcal{P} \subset \mathbb{R}^3 \right\},$$

is, from now on, called **reference configuration**. In the rest of the work the dependence of  $\mathbf{X}(\eta^1, \eta^2, \eta^3)$  is suppressed. We simply write  $\mathbf{X}$  for a point of  $\Omega$ .

The set  $\Omega$  can, for example, describe a component of a mechanical device. The first part of the problem is how this component is deformed under mechanical forces. For a mathematical approach we first need a description of the component after the deformation. Therefore, the set  $\Omega_t$  is introduced, which is described by

$$\Omega_t = \left\{ \mathbf{x}(\eta^1, \eta^2, \eta^3) \mid (\eta^1, \eta^2, \eta^3) \in \mathcal{P} \subset \mathbb{R}^3 \right\}. \quad (5)$$

This configuration describes the mechanical component after the deformation. For a description of the deformation a function  $\Phi : \Omega \rightarrow \Omega_t$  is introduced, which is given by

$$\Phi(\mathbf{X}) = \mathbf{x}.$$

To understand this formula we have to remember that  $\mathbf{X}$  as well as  $\mathbf{x}$  depend on the parameters  $(\eta^1, \eta^2, \eta^3) \in \mathcal{P}$ . Although the deformation is described by  $\Phi$  it is not the function we are interested in. We rather are interested in the information how a point  $\mathbf{X}$  has changed in relation to its position in the reference configuration. Therefore the **displacement vector field**  $\mathbf{u}$  is introduced

$$\mathbf{u} = \Phi(\mathbf{X}) - \mathbf{X} = \mathbf{x} - \mathbf{X}. \quad (6)$$

It is a function of  $\mathbf{X}$  as well as of  $(\eta^1, \eta^2, \eta^3)$ .

## 2.2. Linear elasticity

In the theory of linear elasticity a linear relation between the displacement and the resulting strains is assumed. This relation is given by the **linearised strain tensor**  $\boldsymbol{\varepsilon}(\mathbf{u})$ , which is described through

$$\boldsymbol{\varepsilon}(\mathbf{u}) = \frac{1}{2} \left( \text{Grad} \mathbf{u} + (\text{Grad} \mathbf{u})^\top \right). \quad (7)$$

So,  $\boldsymbol{\varepsilon}(\mathbf{u})$  is a symmetric tensor of second order. Besides the strains in the component we are also interested in the stresses, which occurs. These stresses are in general described by the **Cauchy stress tensor**  $\boldsymbol{\sigma}$ , which is a symmetric second order tensor, too.

In the case of linear elasticity the relation between  $\boldsymbol{\varepsilon}(\mathbf{u})$  and  $\boldsymbol{\sigma}$  is also assumed to be linear, given by a tensor of fourth order  $\boldsymbol{\mathfrak{C}}$ , with

$$\boldsymbol{\sigma} = \boldsymbol{\mathfrak{C}} : \boldsymbol{\varepsilon}(\mathbf{u}). \quad (8)$$

The tensor  $\boldsymbol{\mathfrak{C}}$  is called **material law** or **stiffness tensor**.

Ongoing information about this topic can be found in [Bow10, chapter 2.1].

## 2.3. Linear thermoelasticity

For a thermodynamical approach it is assumed that the linearised strain tensor (7) can be splitted into two parts, i.e.

$$\boldsymbol{\varepsilon} = \boldsymbol{\varepsilon}_M + \boldsymbol{\varepsilon}_T. \quad (9)$$

Here,  $\boldsymbol{\varepsilon}_M$  represents the strain caused by mechanical loads, whereas the second term  $\boldsymbol{\varepsilon}_T$  stands for the strain caused by thermal expansion. This thermal expansion part  $\boldsymbol{\varepsilon}_T$  can be written as

$$\boldsymbol{\varepsilon}_T = \vartheta \mathbf{T},$$

where  $\mathbf{T}$  is a symmetric tensor of second order, the so called **thermal expansion tensor**, and  $\vartheta = \theta - \theta_0$  is the difference between a **reference temperaturefield**  $\theta_0$  and the **recent temperaturefield**  $\theta$ . The thermal expansion tensor  $\mathbf{T}$  describes the expansion behaviour of the material in  $\mathbb{R}^3$ .

Furthermore, the formula for the stress tensor has changed too. Additional to equation (8), a second part, describing thermal effects, is added:

$$\boldsymbol{\sigma} = \boldsymbol{\mathfrak{C}} : \boldsymbol{\varepsilon} + \vartheta \mathbf{M}. \quad (10)$$

In this equation, the symmetric second order tensor  $\mathbf{M}$  is the **stress-temperature tensor**.

Now, we want to get a relation between  $\mathbf{T}$  and  $\mathbf{M}$ . Therefore, it is assumed that the stresses are still only caused by the mechanical strains, i.e. the equation

$$\boldsymbol{\sigma} = \boldsymbol{\mathfrak{C}} : \boldsymbol{\varepsilon}_M \quad (11)$$

holds.



The substitution of  $\boldsymbol{\varepsilon}$  from equation (9) in equation (10) leads to

$$\boldsymbol{\sigma} = \boldsymbol{\mathcal{C}} : \boldsymbol{\varepsilon}_M + \vartheta \boldsymbol{\mathcal{C}} : \mathbf{T} + \vartheta \mathbf{M}.$$

With respect to equation (11) we get the general relation between  $\mathbf{T}$  and  $\mathbf{M}$  by

$$0 = \vartheta \boldsymbol{\mathcal{C}} : \mathbf{T} + \vartheta \mathbf{M} \Rightarrow \mathbf{M} = -\boldsymbol{\mathcal{C}} : \mathbf{T}.$$

Therefore, the formula for the stress tensor is finally:

$$\boldsymbol{\sigma} = \boldsymbol{\mathcal{C}} : (\boldsymbol{\varepsilon} - \vartheta \mathbf{T}). \quad (12)$$

## 2.4. Heat equation

If we assume that the evolution of temperature within the is independent of the deformation of the domain, we can simply look onto heat equation, which is given by:

$$\left. \begin{aligned} c_\rho \rho \frac{\partial}{\partial t} \theta(\mathbf{X}, t) - \text{Div}(\boldsymbol{\kappa}(\mathbf{X}) \cdot \text{Grad} \theta(\mathbf{X}, t)) &= \gamma(\mathbf{X}, t) & \mathbf{X} \in \Omega \\ \theta(\mathbf{X}, 0) &= \theta_0(\mathbf{X}) & \mathbf{X} \in \Omega \\ \frac{\partial}{\partial \mathbf{n}} \theta(\mathbf{X}, t) &= \theta_b & \mathbf{X} \in \Gamma_n, t > 0 \\ \theta(\mathbf{X}, t) &= 0 & \mathbf{X} \in \Gamma_d, t > 0, \end{aligned} \right\} \quad (13)$$

where  $c_\rho$  is the heat capacity,  $\rho$  is the density,  $\boldsymbol{\kappa}$  is the heat conduction tensor,  $\gamma$  represents a heat source and  $\theta_b$  is the heat flow over the boundary. As initial condition the initial temperature field  $\theta_0$  from section 2.3 is used.

From the above equations follows that the temperature difference  $\vartheta$  from (12)i has a time dependency, if we look at the problem (13). This means the subscript  $t$  of the deformed domain  $\Omega_t$  can be interpreted as time dependency, so  $\Omega_t$  represents the deformed domain over time.

But for our purposes we restrict ourselves to the stationary heat equation, i.e. we look onto

$$\left. \begin{aligned} -\text{Div}(\boldsymbol{\kappa}(\mathbf{X}) \cdot \text{Grad} \theta(\mathbf{X})) &= \gamma(\mathbf{X}) & \mathbf{X} \in \Omega \\ \frac{\partial}{\partial \mathbf{n}} \theta(\mathbf{X}) &= \theta_b & \mathbf{X} \in \Gamma_n \\ \theta(\mathbf{X}) &= 0 & \mathbf{X} \in \Gamma_d. \end{aligned} \right\} \quad (14)$$

Note, that we do not longer need  $c_\rho$  and  $\rho$  of the material we want to simulate.

## 3. Special Cases of Linear Thermoelasticity

### 3.1. Isotropic material

In case of isotropic material the mechanical behaviour is fully described by two parameters  $\lambda$  and  $\mu$ , the so called **Lamé parameters**. The material law in this case is well

known to be

$$\mathfrak{C} = \lambda \mathbf{II} + 2\mu \mathfrak{J}, \quad (15)$$

where  $\mathbf{I}$  is the identity tensor of second order and  $\mathfrak{J}$  is given through  $\mathfrak{J} : \mathbf{V} = \mathbf{V}$  for all symmetric  $\mathbf{V} \in \mathcal{T}_2$ . Because of the isotropy of the material the expansion behaviour, as well as the heat conduction, is the same in all directions. Therefore,  $\mathbf{T}$  and  $\boldsymbol{\kappa}$  can be described as

$$\mathbf{T} = \alpha_{\mathbf{b}} \mathbf{I} \quad \text{and} \quad \boldsymbol{\kappa} = \kappa_c \mathbf{I} \quad (16)$$

where  $\alpha_{\mathbf{b}}$  is the thermal expansion coefficient, and  $\kappa_c$  is the heat conduction.

In the special case of isotropic material it is easy to compute the other quantities given in sections 2.2 and 2.3. Therefore, we use the descriptions for  $\mathfrak{C}$  and  $\mathbf{T}$  from the equations (15) and (16). It follows for the stress-temperature tensor

$$\begin{aligned} -\mathbf{M} &= \mathfrak{C} : \mathbf{T} \\ &= (\lambda \mathbf{II} + 2\mu \mathfrak{J}) : \mathbf{T} \\ &= \text{tr}(\mathbf{T}) \lambda \mathbf{I} + 2\mu \mathbf{T} \end{aligned} \quad (17)$$

$$\begin{aligned} &= 3\alpha_{\mathbf{b}} \lambda \mathbf{I} + 2\mu \alpha_{\mathbf{b}} \mathbf{I} \\ &= \alpha_{\mathbf{b}} (3\lambda + 2\mu) \mathbf{I}. \end{aligned} \quad (18)$$

So, with (12) and (15) we get the equation

$$\boldsymbol{\sigma} = \lambda \text{tr}(\boldsymbol{\varepsilon}) \mathbf{I} + 2\mu \boldsymbol{\varepsilon} - \vartheta \alpha_{\mathbf{b}} (3\lambda + 2\mu) \mathbf{I},$$

for the stresses in the linear thermoelastic case.

### 3.2. Transversely isotropic material

In the case of transversely isotropic material it exists a direction at every point  $\mathbf{X} \in \Omega$ , where the material behaves in a different way than perpendicular to this direction. This special direction can be described by a vector field  $\mathbf{a} : \Omega \rightarrow \mathbb{S}^2$  where  $\mathbb{S}^2$  is the unit sphere in  $\mathbb{R}^3$ , i.e.

$$\mathbb{S}^2 = \{ \mathbf{x} \in \mathbb{R}^3 \mid \|\mathbf{x}\|_2 = 1 \}.$$

For the case of transverse isotropy the material law is given through

$$\mathfrak{C} = \lambda \mathbf{II} + 2\mu \mathfrak{J} + \alpha(\mathbf{a}\mathbf{a}\mathbf{I} + \mathbf{I}\mathbf{a}\mathbf{a}) + 2(\mu_{\mathbf{a}} - \mu) \hat{\mathfrak{C}} + \beta \mathbf{a}\mathbf{a}\mathbf{a}\mathbf{a}, \quad (19)$$

which can be found for example in [WM10, chapter 2]. In this formula, the tensor  $\hat{\mathfrak{C}}$  is defined by

$$\hat{\mathfrak{C}} : \mathbf{V} = \mathbf{a}\mathbf{a} \cdot \mathbf{V} + \mathbf{V} \cdot \mathbf{a}\mathbf{a}, \quad \text{for } \mathbf{V} \in \mathcal{T}_2.$$

The transversely isotropic material behaviour is often described by the mechanical constants  $E$ ,  $E_{\mathbf{a}}$ ,  $G$ ,  $G_{\mathbf{a}}$ ,  $\nu$ ,  $\nu_{\mathbf{a}\mathbf{b}}$ , and  $\nu_{\mathbf{b}\mathbf{a}}$ . These quantities are explained in table 3. The

$E$	Elastic modulus
$E_{\mathbf{a}}$	Elastic modulus in direction $a$
$G$	shear modulus
$G_{\mathbf{a}}$	shear modulus in direction $a$
$\nu$	Poisson's ratio in the isotropy plane
$\nu_{\mathbf{ab}}$	Poisson's ratio for pulling in $a$ direction, contraction in the isotropy plane
$\nu_{\mathbf{ba}}$	Poisson's ratio for pulling perpendicular to $a$ , contraction in $a$ direction

Table 3: constants for describing the mechanical behaviour of transversely isotropic material

relation between these constants and the parameters  $\lambda$ ,  $\mu$ ,  $\alpha$ ,  $\mu_{\mathbf{a}}$ , and  $\beta$  from equation (19) can be found in [WM10, chapter 3] and is given by:

$$\left. \begin{aligned} \lambda &= E(\nu + \nu_{\mathbf{ab}}\nu_{\mathbf{ba}})/D \\ \mu &= G \\ \mu_{\mathbf{a}} &= G_{\mathbf{a}} \\ \alpha &= E(\nu_{\mathbf{ab}}(1 + \nu - \nu_{\mathbf{ba}}) - \nu)/D \\ \beta &= (E_{\mathbf{a}}(1 - \nu^2) - E(\nu + \nu_{\mathbf{ab}}\nu_{\mathbf{ba}}) - 2E(\nu_{\mathbf{ab}}(1 + \nu - \nu_{\mathbf{ba}}) - \nu))/D - 4G_{\mathbf{a}} + 2G \end{aligned} \right\} (20)$$

where the divisor  $D$  is described by the equation

$$D = 1 - \nu^2 - 2\nu_{\mathbf{ab}}\nu_{\mathbf{ba}} - 2\nu_{\mathbf{ab}}\nu_{\mathbf{ba}}\nu.$$

Independent of this relation, we note that the first part of  $\mathfrak{C}$  from equation (19) is identical with the isotropic part (15). If the material behaviour in direction  $\mathbf{a}$  is the same as perpendicular to it we are again in the isotropic case from section 3.1. In this case the anisotropic part of  $\mathfrak{C}$  vanishes and only the isotropic part from equation (15) is left over. This can easily be seen by using the equalities

$$E = E_{\mathbf{a}} \quad G = G_{\mathbf{a}} \quad \nu = \nu_{\mathbf{ab}} = \nu_{\mathbf{ba}},$$

which characterise the same behaviour in direction  $\mathbf{a}$  and the isotropy plane. This leads to  $\alpha = \beta = \mu_{\mathbf{a}} - \mu = 0$  (see [WM10, chapter 3]). Thus, equation (15) is only a special case of equation (19).

Of course, besides the changes in the mechanical behaviour, the thermal behaviour is different too. In the direction  $\mathbf{a}$  the thermal expansion, as well as the heat conduction,

is normally different from them in the isotropy plane. Therefore, the thermal expansion tensor  $\mathbf{T}$  and the heat conduction tensor  $\boldsymbol{\kappa}$  can be written as

$$\mathbf{T} = \alpha_{\mathbf{a}}\mathbf{a}\mathbf{a} + \alpha_{\mathbf{b}}(\mathbf{I} - \mathbf{a}\mathbf{a}) = \alpha_{\mathbf{b}}\mathbf{I} + (\alpha_{\mathbf{a}} - \alpha_{\mathbf{b}})\mathbf{a}\mathbf{a}, \quad (21)$$

$$\boldsymbol{\kappa} = \kappa_{\mathbf{a}}\mathbf{a}\mathbf{a} + \kappa_{\mathbf{b}}(\mathbf{I} - \mathbf{a}\mathbf{a}) = \kappa_{\mathbf{a}}\mathbf{b}\mathbf{I} + (\kappa_{\mathbf{a}} - \kappa_{\mathbf{b}})\mathbf{a}\mathbf{a}. \quad (22)$$

Here  $\alpha_{\mathbf{a}}$  is the thermal expansion coefficient in the  $\mathbf{a}$  direction and  $\alpha_{\mathbf{b}}$  is this coefficient in the isotropy plane, as  $\kappa_{\mathbf{a}}$  and  $\kappa_{\mathbf{b}}$  for  $\boldsymbol{\kappa}$ . Analogously to  $\boldsymbol{\mathcal{C}}$ ,  $\mathbf{T}$  and  $\boldsymbol{\kappa}$  consist of an isotropic part and an anisotropic part, dependent on  $\mathbf{a}$ . This part vanishes if the thermal behaviour is the same in direction  $\mathbf{a}$  as perpendicular to it. Again, equation (16) is only a special cases of the equations (21) and (22).

Furthermore, the given representations of  $\mathbf{T}$  and  $\boldsymbol{\kappa}$  can be described intuitively. If we apply the part  $\mathbf{a}\mathbf{a}$  to a first order tensor  $\mathbf{v}$ , then  $\mathbf{a}\mathbf{a} \cdot \mathbf{v}$  is the orthogonal projection onto the direction  $\mathbf{a}$ . This means, that  $(\mathbf{I} - \mathbf{a}\mathbf{a}) \cdot \mathbf{v}$  is the part of  $\mathbf{v}$  in the isotropy plane. This simply means that, when we apply  $\mathbf{T}$  (or  $\boldsymbol{\kappa}$  respectively) to  $\mathbf{v}$

$$\mathbf{T} \cdot \mathbf{v} = \alpha_{\mathbf{a}} \underbrace{\mathbf{a}\mathbf{a} \cdot \mathbf{v}}_{\mathbf{a}\text{-part}} + \alpha_{\mathbf{b}} \underbrace{(\mathbf{I} - \mathbf{a}\mathbf{a}) \cdot \mathbf{v}}_{\text{isotropic part}},$$

that the  $\mathbf{a}$ -part of  $\mathbf{v}$  is multiplied with  $\alpha_{\mathbf{a}}$  (or  $\kappa_{\mathbf{a}}$ ) and the part in the isotropy plane is multiplied with  $\alpha_{\mathbf{b}}$  (or  $\kappa_{\mathbf{b}}$ ). This is exactly the desired behaviour.

## 4. Weak Formulation

The formulas describing a thermoelastic problem are the equilibrium of forces

$$\left. \begin{aligned} \text{Div}\boldsymbol{\sigma}(\mathbf{X}) + f(\mathbf{X}) &= 0 & \mathbf{X} \in \Omega \\ \boldsymbol{\sigma}(\mathbf{X}) \cdot \mathbf{n} &= f_b & \mathbf{X} \in \Gamma_N \\ \mathbf{u} &= 0 & \mathbf{X} \in \Gamma_D \end{aligned} \right\} \quad (23)$$

on the one hand, with  $\Gamma_D \cap \Gamma_N = \emptyset$  and  $\Gamma_D \cup \Gamma_N = \partial\Omega$ , and in our case ( see section 2.4) the stationary heat equation

$$\left. \begin{aligned} \text{Div}(\boldsymbol{\kappa}(\mathbf{X}) \cdot \text{Grad}\vartheta(\mathbf{X})) &= \gamma(\mathbf{X}) & \mathbf{X} \in \Omega \\ \frac{\partial\vartheta}{\partial\mathbf{n}} &= \vartheta_b & \mathbf{X} \in \tilde{\Gamma}_N \\ \vartheta &= 0 & \mathbf{X} \in \tilde{\Gamma}_D \end{aligned} \right\} \quad (24)$$

on the other hand. Analogously, in the problem (24) the relations  $\tilde{\Gamma}_D \cap \tilde{\Gamma}_N = \emptyset$  and  $\tilde{\Gamma}_D \cup \tilde{\Gamma}_N = \partial\Omega$  are valid. A complete derivation of the equations from (23) can be found, for example, in [Bow10, chapter 2.3].

For the weak formulation of problem (23) the equation is multiplied with a test function  $\mathbf{v} \in \mathbb{V}$ , with

$$\mathbb{V} := \left\{ \mathbf{v} \in (\mathbb{H}^1(\Omega))^3 \mid \mathbf{v}(\mathbf{X}) = 0 \quad \forall \mathbf{X} \in \Gamma_D \right\}.$$

After integration by parts, we have

$$\int_{\Omega} \boldsymbol{\sigma} : \boldsymbol{\varepsilon}(\mathbf{v}) \, dV = \int_{\Omega} f \cdot \mathbf{v} \, dV + \int_{\partial\Omega} n \cdot \boldsymbol{\sigma} \cdot \mathbf{v} \, dS.$$

Inserting the Neumann boundary conditions from (23) we finally get

$$\int_{\Omega} \boldsymbol{\sigma} : \boldsymbol{\varepsilon}(\mathbf{v}) \, dV = \int_{\Omega} f \cdot \mathbf{v} \, dV + \int_{\Gamma_N} f_b \cdot \mathbf{v} \, dS.$$

This is the general form of the weak formulation of the equilibrium of forces. Now we substitute (12), and obtain

$$\begin{aligned} \int_{\Omega} (\boldsymbol{\varepsilon}(\mathbf{u}) - \vartheta \mathbf{T}) : \boldsymbol{\mathcal{C}} : \boldsymbol{\varepsilon}(\mathbf{v}) \, dV &= \int_{\Omega} f \cdot \mathbf{v} \, dV + \int_{\Gamma_N} f_b \cdot \mathbf{v} \, dS \\ \int_{\Omega} \boldsymbol{\varepsilon}(\mathbf{u}) : \boldsymbol{\mathcal{C}} : \boldsymbol{\varepsilon}(\mathbf{v}) \, dV - \int_{\Omega} \vartheta \mathbf{T} : \boldsymbol{\mathcal{C}} : \boldsymbol{\varepsilon}(\mathbf{v}) \, dV &= \int_{\Omega} f \cdot \mathbf{v} \, dV + \int_{\Gamma_N} f_b \cdot \mathbf{v} \, dS \\ \int_{\Omega} \boldsymbol{\varepsilon}(\mathbf{u}) : \boldsymbol{\mathcal{C}} : \boldsymbol{\varepsilon}(\mathbf{v}) \, dV &= \int_{\Omega} \vartheta \mathbf{T} : \boldsymbol{\mathcal{C}} : \boldsymbol{\varepsilon}(\mathbf{v}) \, dV + \int_{\Omega} f \cdot \mathbf{v} \, dV + \int_{\Gamma_N} f_b \cdot \mathbf{v} \, dS. \end{aligned}$$

This can be written as

$$a(\mathbf{u}, \mathbf{v}) = b(\mathbf{v}, \vartheta)$$

with a bilinear form  $a$  and a linear functional  $b$  given by

$$a(\mathbf{u}, \mathbf{v}) = \int_{\Omega} \boldsymbol{\varepsilon}(\mathbf{u}) : \boldsymbol{\mathcal{C}} : \boldsymbol{\varepsilon}(\mathbf{v}) \, dV,$$

and

$$b(\mathbf{v}, \vartheta) = \int_{\Omega} \vartheta \mathbf{T} : \boldsymbol{\mathcal{C}} : \boldsymbol{\varepsilon}(\mathbf{v}) \, dV + \int_{\Omega} f \cdot \mathbf{v} \, dV + \int_{\Gamma_N} f_b \cdot \mathbf{v} \, dS.$$

With these two functions (23) is reformulated in a weak sense as:

$$\text{Find } \mathbf{u} \text{ s.t. } a(\mathbf{u}, \mathbf{v}) = b(\mathbf{v}, \vartheta) \quad \forall \mathbf{v} \in \mathbb{V}. \quad (25)$$

We can see that the temperature difference  $\vartheta$  is needed for the description of  $b$ , i. e. we first have to solve (24). It's weak formulation is:

$$\text{Find } \vartheta \text{ s.t. } c(\vartheta, \psi) = \Theta(\psi) \quad \forall \psi \in \mathbb{Q}, \quad (26)$$

with a symmetric bi-linear form  $c$  and a linear functional  $\Theta$  defined by

$$c(\vartheta, \psi) = \int_{\Omega} (\boldsymbol{\kappa} \cdot \nabla \vartheta) \cdot \nabla \psi \, dV,$$

$$\Theta(\psi) = \int_{\Omega} \gamma \psi \, dV + \int_{\Gamma_N} \vartheta_b \cdot \psi \, dS,$$

and the set  $\mathbb{Q}$ , given by

$$\mathbb{Q} = \left\{ \psi \in \mathbb{H}^1(\Omega) \mid \psi(\mathbf{X}) = 0 \quad \forall \mathbf{X} \in \tilde{\Gamma}_D \right\}.$$

These two weak formulations ((25) and (26)) are the starting point for a finite element discretisation.

## 5. Implementation

The material behaviour from section 3.2 was implemented as a module of the software SPC-PM3-AdH, which was developed during the SFB 393. Further information about the general routines can be found in [BMP01]. Additionally, a non-complete list of available modules as well as a detailed description of the general handling of these modules can be found in [Glä09, section 2]. For more information about the used data-structures and the internal structure of the program SPC-PM3-AdH see [Mey14a] and [Mey14b].

The implementation of the module for linear thermoelasticity in case of transverse isotropy based in big parts on merging two other modules. The first module was the module for linear thermoelasticity in the isotropic case, explained in [Glä09, section 2.1]. The second one was the module for transverse isotropy in the linear elastic case, which based on the results from [WM10].

The geometry of the problem is given by a `.std`-file, the structure of which is explained in [Loh98b]. Furthermore the format of the separate blocks in this structure is explained in [Loh98a]. For the usage of the module for thermoelasticity with transverse isotropy, the user has to change the general structure of the `.std`-file on two places. At first, the header has to be fitted to the new module. This done by including the commands `#MAX_MAT_DATA : 17` and `#DEG_OF_FREE : 4` in the header because the number of parameters, which are needed for a description of a material, and the number of the degrees of freedom per node is bigger then the default value. The second change is the `#Material`-block, which consists of 17 parameters. The meaning and the order of the parameters is explained in table 4. In this list the sixth parameter has a special function. It is a switch for choosing isotropic or transversely isotropic material. If this parameter is zero, the parameters 1, 2, 5, 7, 8, 9, 10 and 12 are simply ignored and the isotropic material is defined by the parameters 3, 4, 11 and 13. Nevertheless, the material block has to consist of 17 parameters in this case, too. The right hand sides of the equations (23) and (24) are given elementwise, by defining different materials for elements with different right hand sides. Examples of the material block for different constellations and materials are given in section 6.

This resulting implementation was tested in three steps:

nr.	meaning	nr.	meaning
1	$E_{\mathbf{a}}$ (see Table 3)	9	$\mathbf{a}_3$ ( $x_3$ -component of $\mathbf{a}$ )
2	$\nu_{\mathbf{ab}}$ (see Table 3)	10	$\kappa_a$ (see end of Sec. 3.2)
3	$E$ (see Table 3)	11	$\kappa_b$ (see end of Sec. 3.2)
4	$\nu$ (see Table 3)	12	$\alpha_{\mathbf{a}}$ (thermal exp. coeff. (see Sec. 3.2))
5	$G_{\mathbf{a}}$ (see Table 3)	13	$\alpha_{\mathbf{b}}$ (thermal exp. coeff. (see Sec. 3.2))
6	switch: 0 = isotropic material 1 = transverse isotropic material	14	$f_1$ ( $x_1$ -component of $f$ ) (see (23))
7	$\mathbf{a}_1$ ( $x_1$ -component of $\mathbf{a}$ )	15	$f_2$ ( $x_2$ -component of $f$ ) (see (23))
8	$\mathbf{a}_2$ ( $x_2$ -component of $\mathbf{a}$ )	16	$f_3$ ( $x_3$ -component of $f$ ) (see (23))
		17	$\gamma$ heat source (see (24))

Table 4: meaning of the material parameters in the `.std`-file

- i) comparison of the results in the isotropic case
- ii) test of the thermal behaviour
- iii) comparison with “Abaqus”

In the first step the results for a computation in the isotropic case were compared to the results of the module for linear thermoelasticity for isotropic materials. As explained above the isotropic case can be characterised by two different parameter settings for the material. The first case is to switch the sixth material-parameter to zero. The second way to get isotropic material is choosing an arbitrary direction  $\mathbf{a}$  and set  $E_{\mathbf{a}} = E$ ,  $\nu = \nu_{\mathbf{ab}}$ ,  $G_{\mathbf{a}} = E/(2(1 + \nu))$ ,  $\alpha_{\mathbf{a}} = \alpha_{\mathbf{b}}$ , and  $\kappa_{\mathbf{a}} = \kappa_{\mathbf{b}}$ .

In the next step a problem with  $f \equiv 0$  and  $\gamma \equiv 0$  is formulated, i.e. there are no body forces and no heat sources. The only effect investigated, is the displacement as consequence of the anisotropic expansion behaviour. Therefore the boundary conditions are chosen in such a way that the only appearing effect is thermal expansion.

In the last step a more complex computation was made. The results of this computation were compared to the results of the same problem computed with “Abaqus”, a commercial FEM software.

Some results of these three steps are given in the next section. Furthermore the output of the new module A3D-TEAni in each of the three cases can be found in appendix A.

## 6. Numerical Examples

In this section some results of testing the implementation are presented. Additionally, the parameters used in every example are given with the material blocks from the `.std`-file.

### 6.1. Comparison of the results in the isotropic case

As mentioned at the end of section 5, at first the results in the isotropic case were investigated. For this purpose the example from [Glä09, section 2.1.6] is computed again. Therefore, the material block from the original file `bi.std` was fitted to the new requirements:

```
# MATERIAL: 2
##Nr. 1      2      3 4      5      6 7      8      9      10 11      12      13      14 15 16 17
1 17 0      0      2E2 .3      0      0 0.0 0.0 0.0 0. 1. 0.0      0.001 0. 0. 0. 0.
2 17 2E2 0.3 2E2 .3 76.923077 1 1.0 0.0 0.0 1. 1. 0.005 0.005 0. 0. 0. 10.
```

Each entry starts with the material-number and the number of the material parameters, i.e. the seventeen parameters for describing the material behaviour from table 4 are starting in the third column. For a better understanding the number of the material parameters corresponding to table 4 is shown in the second line. Obviously, material one is assumed as isotropic by switching the sixth parameter to zero. Therefore, the parameters 1, 2, 5, 7, 8, 9,10 and 12 are simply set to zero, because they are ignored. Whereas, material two is isotropic by setting the same material behaviour in the fibre direction as described at the end of section 5.

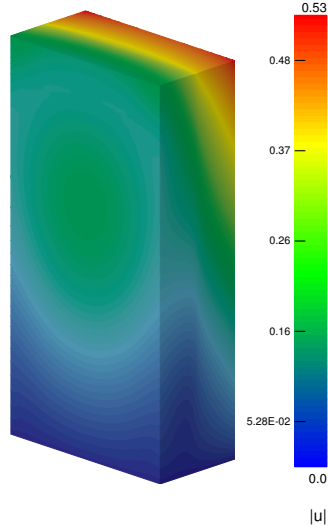


Figure 1: 12 steps, A3D-ThEl

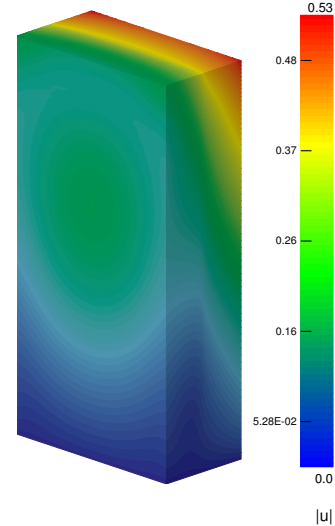


Figure 2: 12 steps, A3D-TEAni

In the Fig. 1 and 2 the computed displacement field after 11 refinement steps is shown. In the left picture we can see the result with the old module A3D-ThEl and on



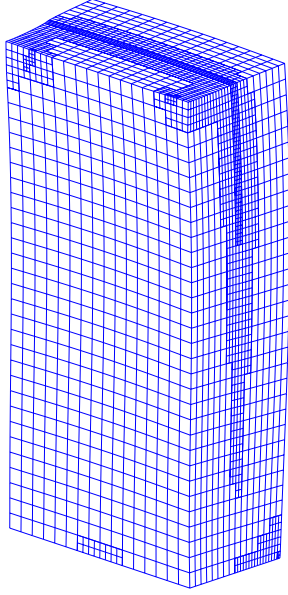


Figure 3: 12 steps, A3D-ThEl

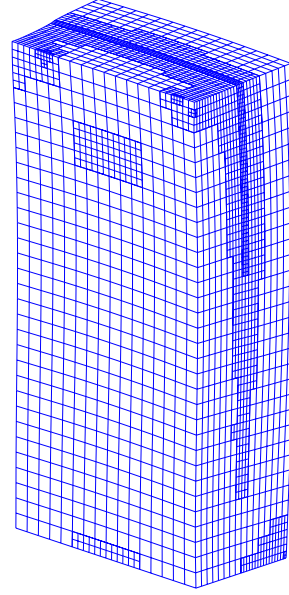


Figure 4: 12 steps, A3D-TEAni

the right hand side the result of the new implementation is shown. There is no apparent difference between the two results.

In the Fig. 3 and 4 are the meshes belonging to the solutions from figures 1 and 2. On the left hand side the mesh after 11 refinement steps is shown, computed with the already existing module A3D-ThEl. Whereas, on the right hand side the mesh with the new implementation is shown after 11 refinement steps. There are some slight differences between these two meshes. The reason therefore are some slight differences in the error estimator. This can be seen in appendix A.1, tables 5 and 6. There is also an explanation for these differences.

## 6.2. Test of the thermal behaviour

For the second step of testing the implementation, the test of the thermal behaviour, a very simple example was treated. This example is a cuboid with the length  $l_1$  in  $x_1$  direction,  $l_2$  in  $x_2$  direction, and  $l_3$  in  $x_3$  direction. Additionally it is assumed that there are perfectly aligned fibres inserted, which causes different material behaviour in the direction they are aligned. So, we have transversely isotropic material. The fibre direction field is given by  $\mathbf{a}(\mathbf{X}) = (1, 0, 0)^\top$ , as can be seen in the schematically description in figure 5.

The boundary conditions are also shown in this figure. There are Dirichlet boundary conditions on three sides of the cuboid, which fix the cuboid in the corner  $(0, 0, 0)$  by

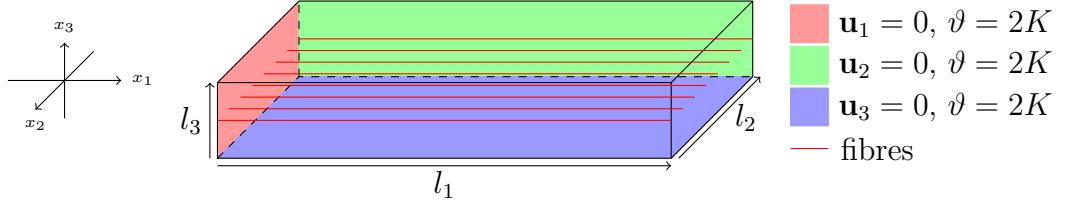


Figure 5: schematic description

setting the corresponding parts of the displacement  $\mathbf{u}$  to zero on these faces. Additionally, the temperature of the cuboid is increased by  $2K$ . So, we can expect that for the displacement within the cuboid the equation

$$\mathbf{u}((x_1, x_2, x_3)^\top) = \vartheta \begin{bmatrix} \alpha_a x_1 \\ \alpha_b x_2 \\ \alpha_b x_3 \end{bmatrix} \quad (27)$$

holds. In the figures 6 to 8 the different components of the displacement for the values

$$\begin{aligned} l_1 &= 4 & \alpha_a &= 0.001 \text{ K}^{-1} \\ l_2 &= 2 & \alpha_b &= 0.005 \text{ K}^{-1} \\ l_3 &= 1 \end{aligned} \quad (28)$$

are shown.

Obviously, the results are exactly what we have expected. The material block for this computation was:

```
# MATERIAL: 1
##Nr.  1   2   3   4   5   6   7   8   9  10  11  12  13  14  15  16  17
1 17  2E2 0.3 2.5E2 .2 1.2E2 1 1.0 0.0 0.0 1.2 1. 0.001 0.005 0. 0. 0. 0.
```

The first five values have no influence on the resulting displacement, because the boundary conditions are chosen in such a way that no mechanical strains occurs. The expansion coefficients from (28) are the 12. and 13. value in this block.

The computational output for the example of this section can be seen in table 7 in section A.2.

### 6.3. Comparison with “Abaqus”

In the last step the results for a more complex example are compared to them from a computation with “Abaqus”, which is a commercial FEM software. Therefore, the behaviour of the component from Fig. 9 is simulated.

The component consist of two layers of transverse isotropic material and different fibre directions  $\mathbf{a}$  for the layers are chosen. In the upper layer the direction is  $\mathbf{a}_u = (1, 0, 0)^\top$  and in the lower layer the direction is  $\mathbf{a}_l = (0, 1, 0)^\top$ . This can be seen in Fig. 10.

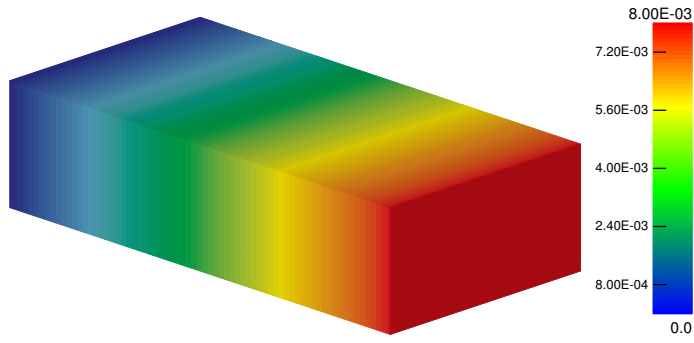


Figure 6:  $\mathbf{u}_1$  in the example from Fig. 5 with the values from (28)

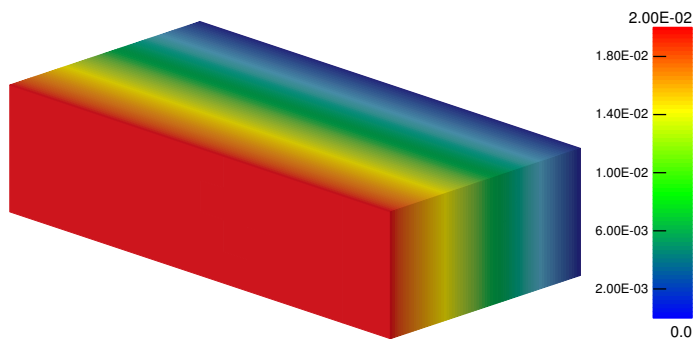


Figure 7:  $\mathbf{u}_2$  in example from Fig. 5 with the values from (28)

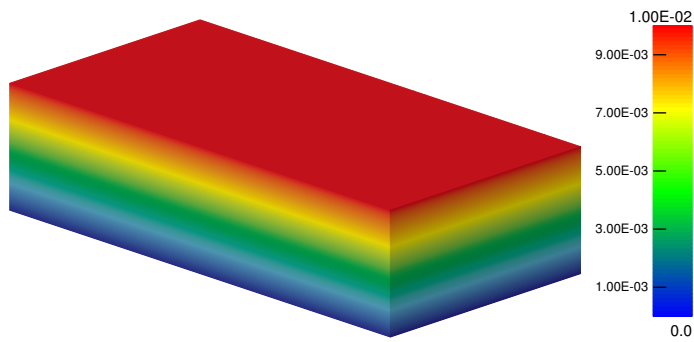


Figure 8:  $\mathbf{u}_3$  in example from Fig. 5 with the values from (28)

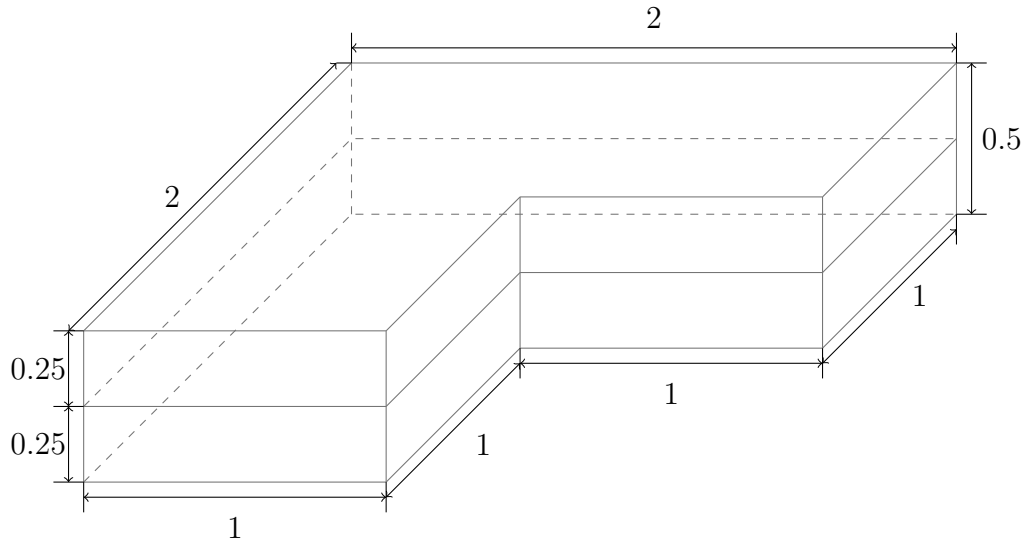


Figure 9: measures of the layered component

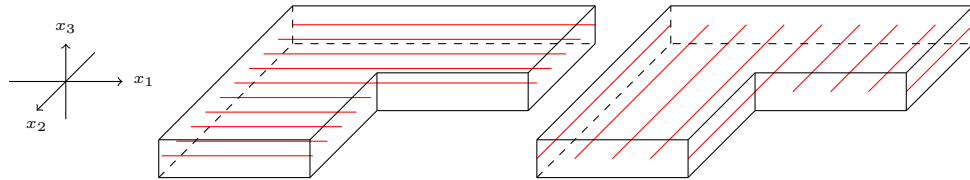


Figure 10: structure of the upper layer (left) and the lower layer (right)

The used boundary conditions for the computation are shown in Fig. 11 and the used material block is

```
# MATERIAL: 2
##Nr.  1   2   3   4   5   6   7   8   9  10  11  12  13  14  15  16  17
1 16  2.5E2 .2  2E2 .3  1.2E2 1  1.0  0.0  0.0  1.2  1.  0.001 0.005 0.  0.  0.  0.
2 16  2.5E2 .2  2E2 .3  1.2E2 1  0.0  1.0  0.0  1.2  1.  0.001 0.005 0.  0.  0.  0.
```

With this material block the used material parameters for both materials are:

$$\begin{array}{lll}
 E_a = 250 \text{ MPa} & E = 200 \text{ MPa} & \kappa_a = 1.2 \\
 \nu_{ab} = 0.2 & \nu = 0.3 & \kappa_b = 1 \\
 G_a = 120 \text{ MPa} & \alpha_a = 0.001 \text{ K}^{-1} & \alpha_b = 0.005 \text{ K}^{-1}
 \end{array}$$

The different material behaviour is caused by the parameters six to nine, which are describing different fibre directions.

The results for this problem with A3D-TEAni, as well as, with “Abaqus” can be seen in Fig. 12. Thanks to Niels Goldberg, for the computation of this problem with

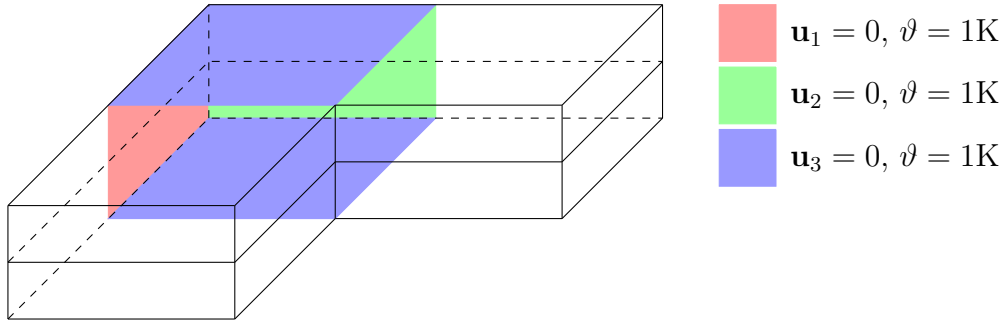


Figure 11: used boundary conditions in the comparison computation

“Abaqus”.

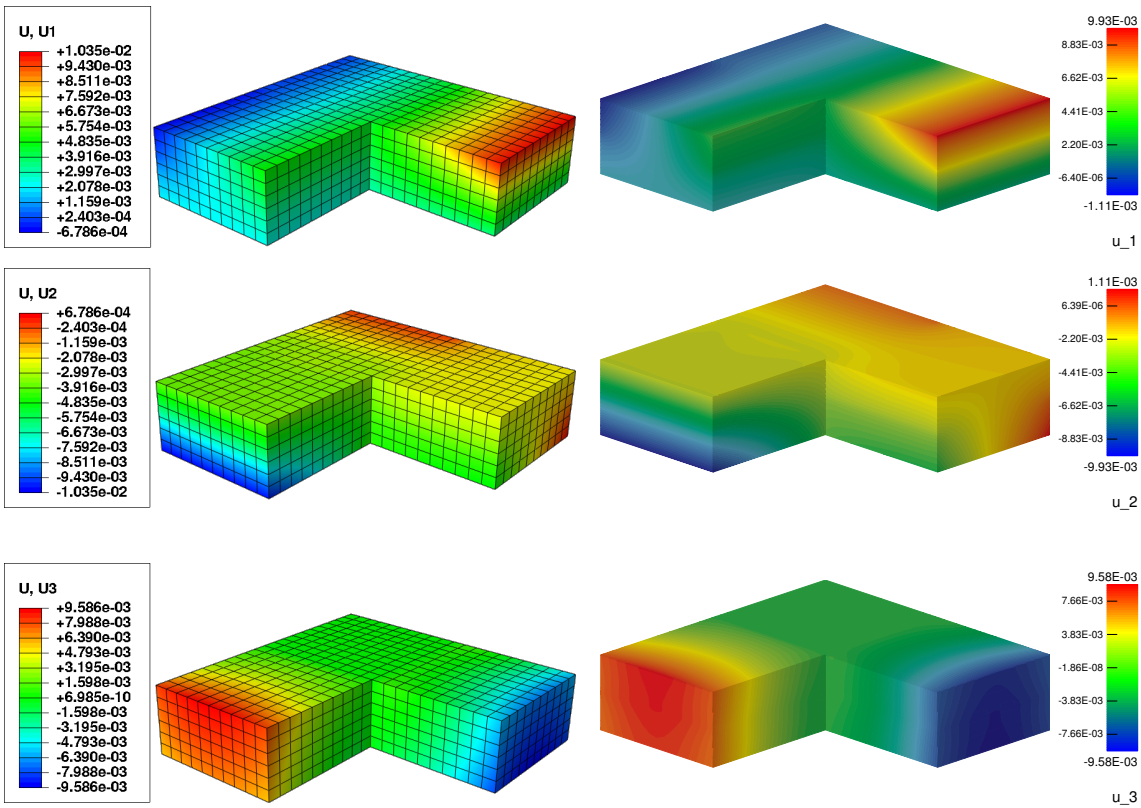


Figure 12: results with “Abaqus” (left) and the new module A3D-TEAni (right)

Obviously, there are some slight differences between the results in the  $x_1$ - and the  $x_2$ -component of the displacement, but the results for the  $x_3$ -component are the same. The differences are likely caused by the adaptivity of our implementation.

The resulting mesh, with the new module can be seen in Fig. 13. There we can see how the mesh was adaptively refined along the interface between the two layers and along the line, where the Dirichlet boundary conditions vanish. These are exact the

areas with the biggest stresses as we see in Fig. 14 or Fig. 15.

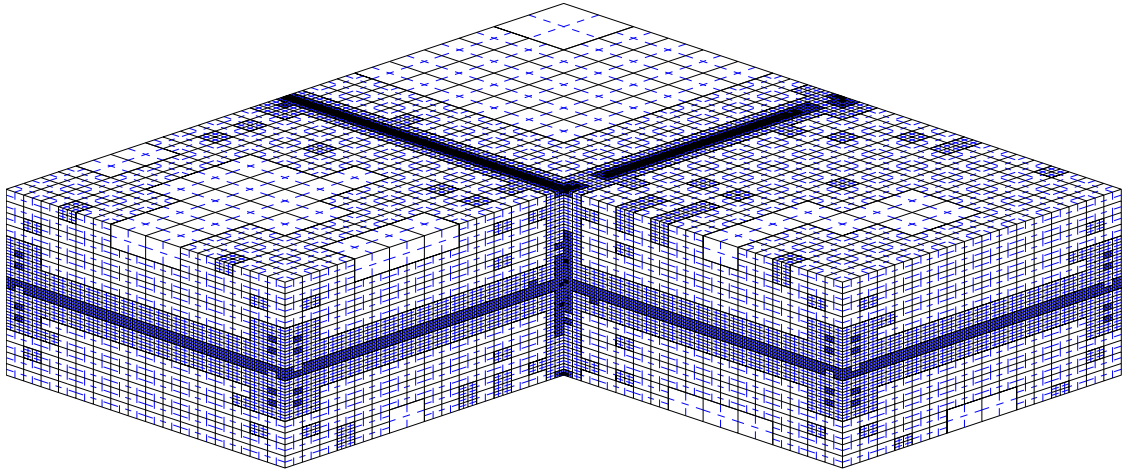


Figure 13: refined net after 14 steps

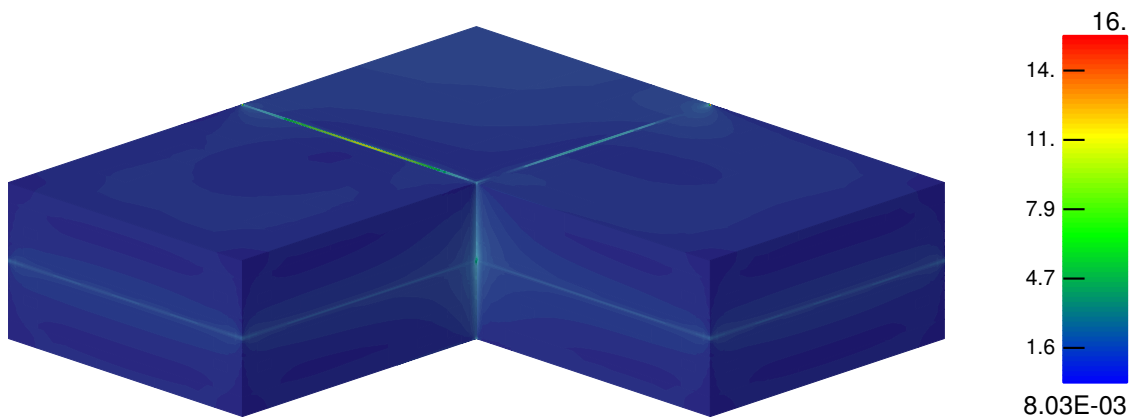


Figure 14: stresses within the component

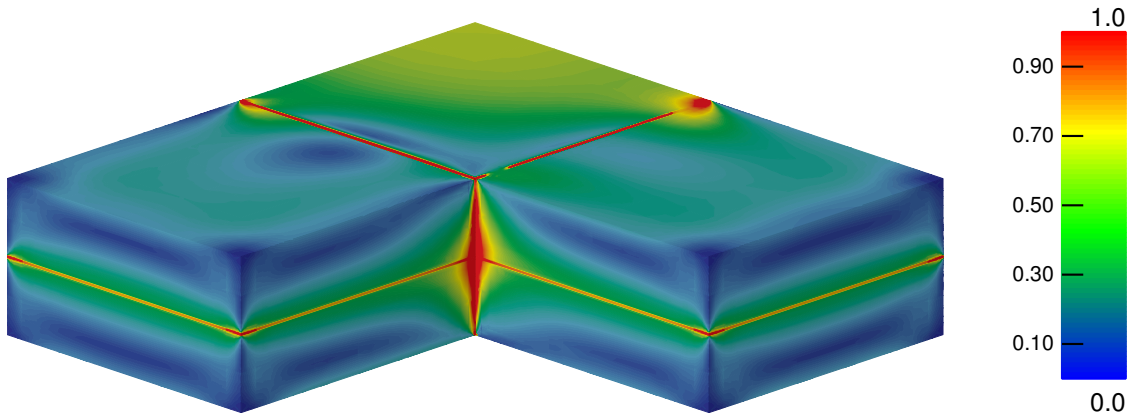


Figure 15: stresses within the component, rescaled

## A. Results of the Computation

### A.1. Comparison of the results in the isotropic case

In this section the results of the re-computation of the problem from [Glä09, Sec. 2.1.6] can be found. In Table 5 we see the results of the computation with the module A3D-ThEl, which already existed, and in Table 6 we see the results of the module A3D-TEAni, where the new aspects were implemented. As we can see, the results at the beginning of the computation (the first 3 steps) are exactly the same inclusive the estimated error. This means the error estimator, which is mainly the one from [Ver97, Sec. 6] was right adopted. After the first three steps the result are slightly different, which is caused in the difference of the computation of the different parts, like for example the element matrices. Additional, the resulting meshes after 11 refinement steps are also slightly different, as we see in Fig. 3 and Fig. 4. These differences are substantiated by the different computation of the error estimator and thereby a different number of marked elements, as we can see in Table 5 and Table 6. Therefore, the resulting mesh contains of a different number of elements. Despite these differences the computation during the two modules is doing the same, as we can see in the Fig. 16 to 18 But despite these differences nearly the same mesh is generated. We also see that the mesh from Fig. 18 lies somewhere between the meshes from Fig. 16 and Fig. 17.

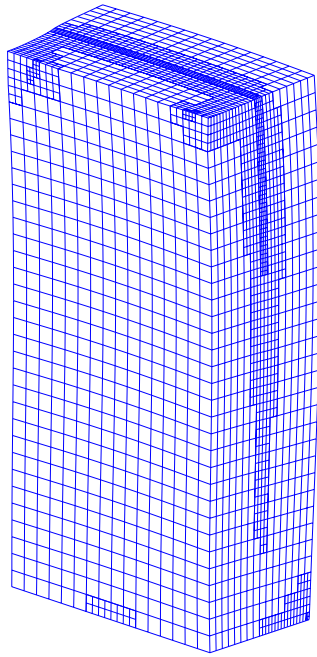


Figure 16: 11 steps,  
A3D-ThEl

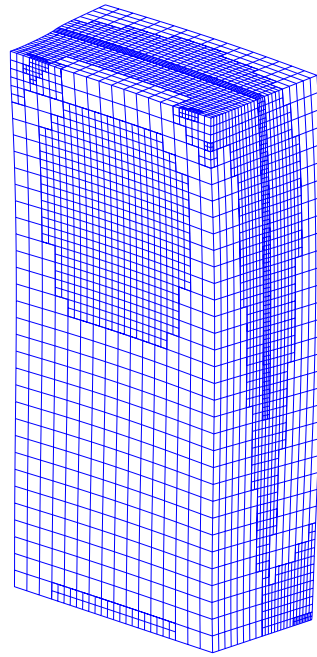


Figure 17: 12 steps,  
A3D-ThEl

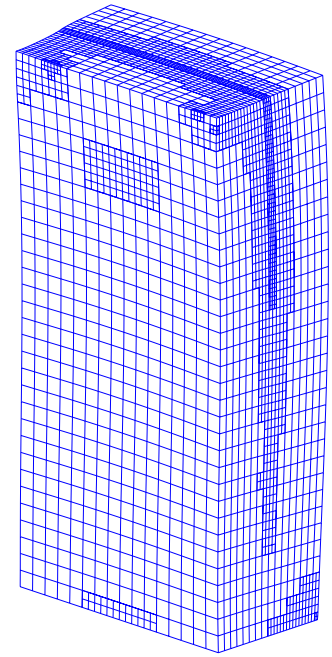


Figure 18: 11 steps,  
A3D-TEAni

NetFine:			Assem :	PCGM			#Elems to ref.	est.Err.
#Nodes	#Elems	#UnKns		time[s]	It	time[s]		
225	16	180	0.002	8	0.000	4.9E + 01	10	1.0E + 00
				2	0.000	1.2E + 02		
979	86	668	0.004	13	0.000	1.0E + 00	6	3.4E - 01
				3	0.002	4.0E + 05		
1433	128	964	0.002	12	0.000	5.5E + 00	19	2.9E - 03
				13	0.004	4.2E - 01		
2923	275	1880	0.004	18	0.000	5.4E - 01	41	2.2E - 01
				13	0.008	3.5E + 01		
5719	562	3548	0.004	13	0.002	3.7E + 00	36	1.5E - 01
				19	0.020	3.1E + 00		



NetFine:			Assem :	PCGM			#Elems to ref.	est.Err.
#Nodes	#Elems	#UnKns		time[s]	It	time[s]		
7821	814	4632	0.004	22	0.008	1.5E + 00	50	1.2E - 01
				20	0.031	2.4E + 00		
11395	1164	6860	0.012	13	0.023	6.8E - 01	64	9.8E - 02
				19	0.035	1.5E + 00		
15941	1619	9628	0.016	15	0.023	2.5E - 01	241	8.6E - 02
				15	0.039	4.2E + 00		
31035	3341	17844	0.023	15	0.027	5.5E - 01	345	5.9E - 02
				21	0.082	1.7E + 00		
52483	5791	29528	0.039	19	0.059	3.7E - 01	523	4.0E - 02
				26	0.129	1.2E - 01		
85467	9452	48028	0.063	16	0.078	3.3E - 01	293	2.8E - 02
				26	0.203	1.3E - 01		
167197	18685	93044	0.125	32	0.270	1.4E - 01	2614	2.1E - 01
				26	0.371	6.3E - 02		

Table 5: results of the computation with the module A3D-ThEl

NetFine:			Assem :	PCGM			#Elems to ref.	est.Err.
#Nodes	#Elems	#UnKns		time[s]	It	time[s]		
225	16	180	0.008	8	0.008	4.9E + 01	8	1.0E + 00
				2	0.012	1.2E + 02		
979	86	668	0.000	13	0.004	1.0E + 01	6	3.4E - 01
				3	0.002	4.0E + 05		
1433	128	964	0.008	12	0.027	5.5E + 00	19	2.9E - 01
				13	0.004	4.2E + 01		

NetFine:			Assem :	PCGM			#Elems to ref.	est.Err.
#Nodes	#Elems	#UnKns		time[s]	It	time[s]		
2923	275	1880	0.004	18	0.000	5.4E - 01	38	2.2E - 01
				12	0.004	6.1E + 01		
5519	541	3436	0.004	13	0.004	3.5E + 00	39	1.6E - 01
				21	0.027	1.4E + 00		
7821	814	4632	0.008	21	0.012	1.6E + 00	51	1.2E - 01
				17	0.008	6.1E + 00		
11477	1171	6916	0.016	13	0.020	6.8E - 01	79	9.8E - 02
				16	0.031	3.9E + 00		
16989	1738	10200	0.020	19	0.027	3.6E - 01	261	8.3E - 02
				14	0.039	9.7E + 00		
33261	3607	19008	0.031	14	0.035	4.8E - 01	369	5.6E - 02
				24	0.102	5.1E - 01		
56193	6211	31548	0.051	20	0.070	3.7E - 01	372	3.7E - 02
				21	0.117	2.3E - 01		
79415	8815	44500	0.066	17	0.066	2.7E - 01	1875	2.9E - 02
				22	0.156	2.4E - 01		
196149	22059	108540	0.176	30	0.320	1.7E - 01	2957	1.9E - 02
				23	0.371	1.3E - 01		

Table 6: results of the computation with the module A3D-TEAni

## A.2. Test of the thermal behaviour

In this section the output for the computation of the example from Sec. 6.2 is shown. As seen in (27) the displacement in this example is a linear function over our domain  $\Omega$ . Therefore, the exact solution is a part of the discretized FE space  $V_h$ , which is not the case in general. But in this setting, it means that the solution can be computed exactly.

This can also be seen in the results of the error estimator in the last column of Table 7. There we see that the estimated error is nearly zero after the first one/two refinement

steps, which means that we already have the exact solution.

NetFine:			Assem :	PCGM			#Elems to ref.	est.Err.
#Nodes	#Elems	#UnKns		time[s]	It	time[s]		
135	8	120	0.000	3	0.000	2.0E + 01	3	2.6E - 05
				2	0.000	7.9E - 01		
397	29	308	0.000	5	0.000	2.8E - 03	9	1.3E - 09
				7	0.000	1.2E - 05		
1095	92	768	0.008	6	0.029	3.2E - 08	17	7.5E - 14
				9	0.002	5.4E - 10		
2449	211	1676	0.002	6	0.002	8.2E - 13	23	1.4E - 15
				11	0.002	3.3E - 14		
5479	505	3572	0.006	8	0.002	1.2E - 29	27	4.3E - 15
				9	0.004	2.7E - 14		
10517	988	6748	0.008	9	0.021	1.6E - 29	87	8.3E - 15
				9	0.008	3.6E - 14		
21877	2171	13448	0.023	10	0.010	2.3E - 29	168	1.1E - 14
				9	0.039	6.5E - 14		
48973	4880	30008	0.039	10	0.029	3.6E - 29	72	2.3E - 14
				9	0.070	9.1E - 14		
61277	1219	37324	0.041	11	0.043	4.0E - 29	34	2.7E - 14
				9	0.074	7.6E - 14		
66313	6665	40364	0.021	11	0.045	4.4E - 29	293	2.9E - 14
				9	0.076	6.3E - 14		
116269	11803	70292	0.096	15	0.105	5.8E - 29	971	4.1E - 14
				9	0.104	1.6E - 13		

Table 7: results of the computation for testing the thermal behaviour

### A.3. Results of A3D-TEAni in the comparison computation

In the following table the results for the computation of the example from section 6.3 are shown.

#Nodes	NetFine:		Assem : time[s]	PCGM			#Elems to ref.	est.Err.
	#Elems	#UnKns		It	time[s]	<r,w>		
325	24	1300	0.008	12	0.016	2.8E + 01	12	6.0E - 02
				10	0.008	1.5E - 02		
1241	108	4964	0.023	11	0.016	1.1E - 03	14	3.5E - 02
				17	0.008	3.3E - 05		
2313	206	9252	0.031	16	0.000	1.4E - 07	10	2.6E - 02
				17	0.039	2.0E - 05		
3057	276	12228	0.031	12	0.008	1.4E - 11	20	1.8E - 02
				16	0.039	6.9E - 06		
4581	416	18324	0.055	10	0.008	1.1E - 11	39	1.6E - 02
				19	0.055	5.0E - 06		
7523	689	30092	0.094	10	0.016	1.5E - 11	99	1.4E - 02
				20	0.078	4.6E - 06		
14571	1389	58284	0.188	10	0.023	4.5E - 11	76	1.0E - 02
				20	0.125	6.5E - 06		
19707	1935	78828	0.258	10	0.023	3.7E - 11	179	7.5E - 03
				22	0.195	1.7E - 06		
32789	3188	131156	0.438	10	0.039	4.4E - 11	304	5.4E - 03
				23	0.328	2.4E - 06		
54705	5344	218820	0.719	10	0.078	4.0E - 11	262	3.9E - 03
				23	0.477	2.1E - 06		
73357	7206	293428	0.945	10	0.109	5.9E - 11	952	3.2E - 03
				23	0.648	6.5E - 07		
140993	13912	563972	1.824	10	0.242	1.7E - 10	1067	2.1E - 03
				26	1.492	1.1E - 06		

NetFine:			Assem :	PCGM			#Elems to ref.	est.Err.
#Nodes	#Elems	#UnKns		time[s]	It	time[s]		
214313	21451	857252	2.844	10	0.703	1.7E - 10	481	1.6E - 03
				27	2.633	4.3E - 07		
246293	24994	985172	1.875	10	0.430	1.1E - 10	430	1.3E - 03
				22	2.867	9.3E - 08		
275101	27982	1100404	1.633	10	0.609	7.2E - 11	208	1.2E - 03
				25	3.617	7.6E - 08		

Table 8: results of the computation of the example from section 6.3

## References

- [BMP01] Sven Beuchler, Arnd Meyer, and Matthias Pester. SPC-PM3AdH v1.0 - Programmer's Manual. Preprint SFB/393 01-08, TU-Chemnitz, 2001.
- [Bow10] Allan F. Bower. Applied Mechanics of Solids. CRC Press, 2010.
- [Glä09] Janine Glänzel. Kurzvorstellung der 3D-FEM Software SPC-PM3AdH-XX. Preprint CSC 09-03, TU-Chemnitz, 2009.
- [Loh98a] Dag Lohse. Ein Standard-File für 3D-Gebietsbeschreibungen - Datenbasis und Programmschnittstelle data\_read. Preprint SFB/393 98-17, TU-Chemnitz, 1998.
- [Loh98b] Dag Lohse. Ein Standardfile für 3D-Gebietsbeschreibungen. Preprint SFB/393 98-11, TU-Chemnitz, 1998.
- [Mey14a] Arnd Meyer. Programmbeschreibung SPC-PM3-AdH-XX, Teil 1. Preprint CSC 14-01, TU-Chemnitz, 2014.
- [Mey14b] Arnd Meyer. Programmbeschreibung SPC-PM3-AdH-XX, Teil 2. Preprint CSC 14-02, TU-Chemnitz, 2014.
- [Ver97] Rüdiger Verfürth. A Review of A Posteriori Error Estimation Techniques for Elasticity Problems. 1997.
- [WM10] Michael Weise and Arnd Meyer. Grundgleichungen für transversal isotropes Materialverhalten. Preprint CSC 10-02, TU-Chemnitz, 2010.

Some titles in this CSC and the former SFB393 preprint series:

- 10-01 A. Meyer, P. Steinhorst. Modellierung und Numerik wachsender Risse bei piezoelektrischem Material. May 2010.
- 10-02 M. Balg, A. Meyer. Numerische Simulation nahezu inkompressibler Materialien unter Verwendung von adaptiver, gemischter FEM. Juni 2010.
- 10-03 M. Weise, A. Meyer. Grundgleichungen für transversal isotropes Materialverhalten. Juli 2010.
- 10-04 M. K. Bernauer, R. Herzog. Optimal Control of the Classical Two-Phase Stefan Problem in Level Set Formulation. October 2010.
- 11-01 P. Benner, M.-S. Hossain, T. Stykel. Low-rank iterative methods of periodic projected Lyapunov equations and their application in model reduction of periodic descriptor systems. February 2011.
- 11-02 G. Of, G. J. Rodin, O. Steinbach, M. Taus. Coupling Methods for Interior Penalty Discontinuous Galerkin Finite Element Methods and Boundary Element Methods. September 2011.
- 12-01 J. Rückert, A. Meyer. Kirchhoff Plates and Large Deformation. April 2012.
- 12-02 A. Meyer. The Koiter shell equation in a coordinate free description. February 2012.
- 12-03 M. Balg, A. Meyer. Fast simulation of (nearly) incompressible nonlinear elastic material at large strain via adaptive mixed FEM. July 2012.
- 13-01 A. Meyer. The Koiter shell equation in a coordinate free description – extended. September 2013.
- 13-02 R. Schneider. With a new refinement paradigm towards anisotropic adaptive FEM on triangular meshes. September 2013.
- 13-01 A. Meyer. The linear Naghdi shell equation in a coordinate free description. November 2013.
- 14-01 A. Meyer. Programmbeschreibung SPC-PM3-AdH-XX – Teil 1. März 2014.
- 14-02 A. Meyer. Programmbeschreibung SPC-PM3-AdH-XX – Teil 2. .
- 14-03 J. Glänzel, R. Unger. High Quality FEM-Postprocessing and Visualization Using a Gnuplot Based Toolchain. July 2014.
- 14-04 M. Weise. A note on the second derivatives of rHCT basis functions. October 2014.

The complete list of CSC and SFB393 preprints is available via  
<http://www.tu-chemnitz.de/mathematik/csc/>



